Spatial Resolution Correction for Electrochemical Wall-shear Stress Measurements using Rectangular Sensors

Fawzi Fadla, Rogelio Chovet, Denis Cornu, Marc Lippert, Fethi Aloui, Laurent Keirsbulck

Journal of Applied Fluid Mechanics , Vol. 9, No. 3, pp. 1309-1319, 2016.
Available online at www.jafmonline.net, ISSN 1735-3572, EISSN 1735-3645.
DOI: 10.18869/acadpub.jafm.68.228.23945

Spatial Resolution Correction for Electrochemical Wall-shear Stress Measurements using Rectangular Sensors

F. Fadla[2], R. Chovet[1], D. Cornu[1], M. Lippert[1], F. Aloui[1†] and L. Keirsbulck[1]

[1] LAMIH CNRS UMR 8201, UVHC, *Univ. Lille Nord de France, F-59313, Valenciennes, France*
[2] *Laboratory of Fluid Mechanics,* EMP, *BP 17 Bordj El Bahri, Alger, Algérie*

† *Corresponding Author Email*: *fethi.aloui@univ-valenciennes.fr*

(Received Julay 14, 2014; accepted January 7, 2015)

ABSTRACT

This article is mainly motivated by the growing needs for highly resolved measurements for wall-bounded turbulent flows and aims to proposes a spatial correction coefficient in order to increase the wall-shear stress sensors accuracy. As it well known for the hot wire anemometry, the fluctuating streamwise velocity measurement attenuation is mainly due to the spatial resolution and the frequency response of the sensing element. The present work agrees well with this conclusion and expands it to the wall-shear stress fluctuations measurements using electrochemical sensors and suggested a correction method based on the spanwise correlation coefficient to take into account the spatial filtering effects on unresolved wall-shear stress measurements due to too large sensor spanwise size.

Keywords: Spatial resolution; Wall-shear stress measurements; Electrochemical method; Inverse method.

NOMENCLATURE

C	active ion concentration in the layer		wall
		$\overline{S}$	average velocity gradient at the wall
C_0	active ion concentration (in solution)	Sh	Sherwood number
$\mathcal{D}$	diffusion coefficient	U	mean velocity
f^*	dimensionless frequency	u'	fluctuating velocity
h	channel height	u_τ	friction velocity
subscript m	denote the measured value	x	streamwise direction
subscript r	denote the real value	y	normal direction
subscript c	denote the corrected value	z	spanwise direction
l	sensor length		
supercript $+$	inner scaling (using u_τ and ν)	$\overline{\tau}$	mean wall-shear stress
subscript $*$	dimensionless value (mass transfer)	τ'	fluctuating wall-shear stress
		ν	cinematic vicosity
Pe	Péclet number	δ_c	diffusion thickness
R	spanwise correlation coefficient	ξ_z	spanwise shift
$Re_\tau = h^+/2$	Kármán number	α	correction coefficient
S	velocity gradient at the	λ	constant parameter

1. INTRODUCTION

So far, there is no consensus about wall-shear stress statistics of wall-bounded flows (e.g., pipe, channel and boundary layer)(Buschmann and Gad-el-Hak 2010; Monty *et al.* 2009; Monty *et al.* 2009), the Reynolds number dependency of such quantities is not fully explained yet (Wu and Moin 2010). These dependencies are still a controversial topic, although many investigators have been studying

wall-bounded flow (Alfredsson *et al.* 1988; Durst *et al.* 1996; Degraaff and Eaton 2000; Morrison *et al.* 2004; Hutchins and Marusic 2007; Hultmark *et al.* 2010). The physical reason is not clearly understood and need to have access to well resolved measurements in wall-bounded turbulent flows and especially in the near wall region. But in the literature, some discrepancies between experimental and numerical data of such flows have still observed and reported by different groups of researchers (Fischer *et al.* 2001; Örlü *et al.* 2010). It is now well known that these discrepancies observed between high-resolved direct numerical simulation and experimental velocities statistics could be explained and are attributed to unresolved experimental measurements. In a recent letter, Örlü and Schlatter (Örlü and Schlatter 2011) demonstrated that this discrepancy is linked to the spatial resolution effects using spanwise filtering DNS Data in order to mimic the experimental measurements limited in spatial resolution. A spatial filtering over small flow scales may occurs when the length of the probe used to measure turbulent quantities close to the wall is larger than the size of these turbulent small scales. Clear attenuation of the small-scale DNS energy was observed as the filter length was increased and good agreement was noted with hot-wire experiments from Österlund thesis (Österlund 1999) over a range of sensing lengths up to $l^+ = 60$, where l is the sensor length and the inner scaling is denoted by $+$ superscript. Insufficient spatial resolution is known to affect hot-wire measurements accuracy and could account for some discrepancies in published results also mentioned in the well-known and well-cited study of Ligrani and Bradshaw (Ligrani and Bradshaw 1987). Consequently, hot wire anemometry (HWA) measurements spatial resolution could be explained the main difference between DNS and experimental velocities statistics in the near wall region especially for high Reynolds numbers. Most experimental studies on the topic used these popular techniques that generally displays a very low spatial resolution due to the relatively large spanwise measuring volume or sensing length (Cameron *et al.* 2010). Unresolved velocity measurements in turbulent flows close to walls resulting from the finite size of a hot-wire probe can be however corrected. A number of correction schemes are available in the literature over the last ten years, based on heuristic curve fitting (Monkewitz *et al.* 2010; Hutchins *et al.* 2009) or physical models (Talamelli *et al.* 2013; Smits *et al.* 2011; Segalini *et al.* 2013). With regard to its progress to obtained well resolved turbulent velocities statistics, only few studies are devoted to direct wall-shear stress measurements. For example, the classical way to determine the relative wall-shear stress fluctuation is generally not based on direct wall-shear stress measurements, but on an asymptotic behavior of velocities measurement as follows:

$$\lim_{y^+\to 0} \frac{\sqrt{\overline{u'^{2+}}}}{U^+} = \frac{\sqrt{\overline{\tau'^2}}}{\bar{\tau}} \tag{1}$$

with U, the mean velocity, u', the fluctuating velocity, $\bar{\tau}$, the mean wall-shear stress, τ', the fluctuating wall-shear stress and y, the distance from the wall. So, another possibility to explain the systematic departure of the experimental wall-shear stress fluctuation compared to the DNS, could be also accounted by the accuracy of the values found from the limiting behavior of the turbulence intensity that are slightly under-estimated. Indeed, velocity measurements suffer from a lack of accuracy close to the wall, especially due to the wall heat transfer phenomena for HWA measurements. Of the several methods available for the direct time-series measurement of wall-shear stress, the hot-film sensor is perhaps the most widespread Chew *et al.* (1998). As also mentioned by Örlü and Schlatter (Örlü and Schlatter 2011), there has been considerable progress over the last decade in innovative techniques to measure directly the mean and especially fluctuating wall-shear stress (Naqwi and Reynolds 1991; Miyagi *et al.* 2000; Brücker*et al.* 2005). Nevertheless, the main problem of these pointed techniques is the poor frequency response and there is still room for improvement. In order to discuss the anomalous decrease in overall experimental statistical wall measurements, the electrochemical method (see Hanratty and Campbell (Hanratty and Campbell 1996) for a thorough review), based on the determination of the limiting diffusion current at the surface of an electrode, is used to provide information on the wall-shear stress fluctuations. We also proposed to expand the theoretical correction for non-uniform flow, introduced by Mitchell and Hanratty (Mitchell and Hanratty 1966) based on the spanwise correlation coefficient to take into account the spatial filtering effects on the wall-shear stress measurements.

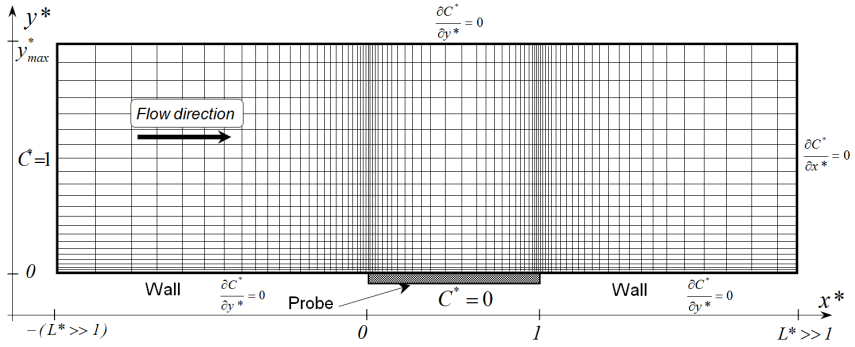

Fig. 1. Boundary conditions for the numerical solution of Eq. 3 on the study control area (L^*, y^*_{max}).

2. INVERSE METHOD FOR THE DETERMINATION OF THE WALL SHEAR STRESS

In the presence of an inert electrolyte in excess, the governing mass transfer equation, in the case of a two-dimensional flow (xy plan), and assuming further that the mass boundary layer is very small compared to the viscous boundary layer, can be written as:

$$\frac{\partial C}{\partial t}+yS(x,t)\frac{\partial C}{\partial x}-\frac{y^2}{2}\frac{\partial S}{\partial x}\frac{\partial C}{\partial y}=\mathcal{D}\Big(\frac{\partial^2 C}{\partial x^2}+\frac{\partial^2 C}{\partial y^2}\Big) \quad (2)$$

where

$$S(x,t)=\frac{\partial U}{\partial y}\Big|_{y=0}$$

is the wall shear stress, C the concentration of the active species and $\mathcal{D}$ the diffusion coefficient.

Most of the works assume that $S(x,t)=S(t)$ over the study control volume. This assumption remains valid if the integration domain is small compared to the spatial scales of the flow. In these conditions, Eq. 2 becomes using dimensionless quantities:

$$f^*Pe^{-2/3}\frac{\partial C^*}{\partial t^*}+y^*S^*\frac{\partial C^*}{\partial x^*}=Pe^{-2/3}\frac{\partial^2 C^*}{\partial x^{*2}}+\frac{\partial^2 C^*}{\partial y^{*2}} \quad (3)$$

where : $x^*=x/l$, $y^*=y/\delta_c$, $t^*=t.f$, $C^*=C/C_0$, $S^*=S/\overline{S}$, l is the width of the electrode (probe), $\overline{S}$ is the mean wall shear stress and with,

$$\delta_c=\Big(\frac{l.\mathcal{D}}{\overline{S}}\Big)^{1/3},\quad f^*=f\frac{l^2}{\mathcal{D}},\qquad Pe=\overline{S}\frac{l^2}{\mathcal{D}}$$

are respectively, the diffusion thickness, the dimensionless frequency and the Péclet number. The Sherwood number (Sh), which is a dimensionless measured limiting diffusion current, is defined as:

$$Sh(t)=Pe^{1/3}\int_0^1\Big(\frac{\partial C^*}{\partial y^*}\Big)_{y^*=0}dx^* \quad (4)$$

In steady regime, by neglecting the tangential distribution for high Péclet numbers, Eq. 3 can be written as:

$$y^*S^*\frac{\partial C^*}{\partial x^*}=\frac{\partial^2 C^*}{\partial y^{*2}} \quad (5)$$

This equation has a dimensionless analytical solution (Mitchell and Hanratty (1966)) as follow:

$$Sh=0.807Pe^{1/3} \quad (6)$$

This solution is commonly referred to Lévêque solution, where Sh denotes the Nusselt mass number, commonly called Sherwood number. In the case of small flow fluctuations, the use of this relationship in quasi-steady regime remains involved. However, if the amplitude of these fluctuations becomes important, solution of Eq. 3 is substantially different from that known as quasi-steady one. Therefore, it appears a phase shift, an attenuation of the amplitude (compared to the real one) and the appearance of higher order harmonics. All these phenomena are due to a capacitive effect caused mainly by the mass boundary layer. In our case, Eq. 3 was solved numerically using the finite volume method. An implicit approach with upwind scheme was used on time with a structured and variable mesh. This mesh was tight in the vicinity of the probe boundary, where the concentration varies a lot, near the wall, and progressively relaxed elsewhere. The boundary conditions for the numerical solution, are shown in Fig. 1.

After a direct solving of Eq. 3 starting from a known wall shear stress, the concentration field is therefore used to calculate the Sherwood number. The numerical integration of this Sherwood number was done using the Simpson method (accurate method) on more than 100 cells along the probe surface (along x^*).

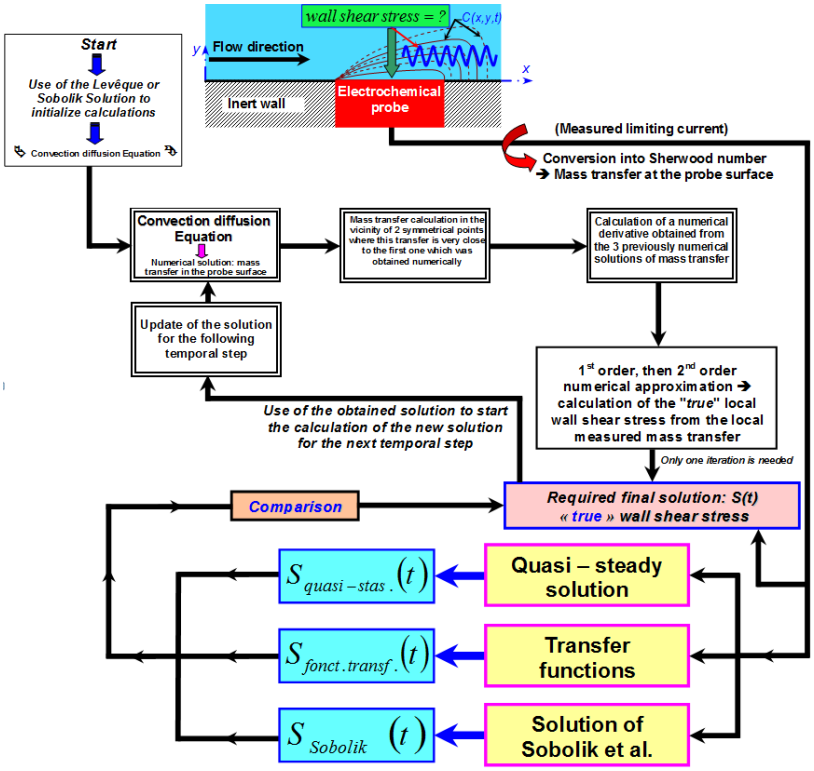

Fig. 2. Flow sheet of the inverse method.

In fact, the inertia of the concentration boundary layer manifests itself in flows with variable wall shear stresses. Due to the low molecular diffusivity of the species which compose the electro-diffusional solution, the limiting diffusion current exhibits a phase shift and smaller amplitude than in the case without inertia (Ambari *et al.* 1985). This inertia is one of the limiting factors of electro-diffusion method (Tihon, Legrand, and Legentilhomme 1995; Sobolik*et al.* Sobolik *et al.*1987). Thus, the true wall shear stress S evaluation from the measured limiting diffusion current (or dimensionless current Sh), cannot be easily obtained because of the big nonlinearity between S and Sh, especially when fluctuations are important. Only, a linearization between Sh and S (assuming many hypotheses: permanent regime or very small wall shear stress fluctuations, high Péclet numbers, and so on...) can be used to transform measured limiting current into wall velocity gradient (Ambari *et al.* 1985; Sobolik*et al.* Sobolik *et al.*1987).

In practice, the direct problem (direct numerical solution of the convection-diffusion equation) cannot be useful for us, because we measure a mass transfer (Sherwood number) from which we must determine the wall shear stress. Thus, we must inverse the convection-diffusion equation in order to find a wall velocity gradient S from a measured Sherwood number (mass transfer) Sh. Indeed, Eq. 3 cannot be inversed neither analytically, nor numerically. Only a numerical specific procedure can be used to approach this inversion, using the called indirect problem or inverse method. The inverse problem (Mao and Hanratty 1991; Rehimi *et al.* 2006), takes into account of the inertia parameter. The principle of this method is well described for the heat conduction problems (Chantasiriwan 1999; Tortorelli and Michaleris 1994; Chantasiriwan 2001; Beck *et al.* 1985). Until recently, the analysis of the wall shear stress from mass transfer measurement used linear approaches (Lévêque quasi-steady method and transfer functions). Furthermore, the majority of the studied cases were validated under a specific hypothesis (for a specific range of Péclet numbers (Ling 1963) or a specific range of oscillation frequencies (Sobolik *et al.* 1986), neglecting also the gap effect (Dumaine 1981). An important consideration was therefore considered for the inverse method using the the polarography technique, by taking into account of the frequencies effect, the inertia on the probe (axial diffusion effect) and the angle effect (using tri-segmented probe). This inverse method was validated in some practical situations (Berrich *et al.* 2011).

The inversion is based on the minimization of the difference between the experimental measurements (Sherwood numbers) and those calculated from convection-diffusion equation. By minimizing this gap, we can obtain the desired functional. In our case, we want to minimize the gap between measurements of limiting diffusion current converted into experimental Sherwood numbers, and mass transfer obtained numerically using the convection-diffusion equation for the same conditions. The objective is to find the true wall shear stress. To minimize the difference between the numbers of Sherwood measured and calculated, we must inverse the convection diffusion equation (Rehimi *et al.* 2006).

The application of an inverse method to the mass transfer problems is original. This method carries numerical inversion of the convection diffusion equation, which cannot be reversed analytically, in order to obtain the true wall shear stress in the case of unsteady flows. In our case, the inverse method is based on a sequential estimation in order to simulate the response of electro-diffusion probe to a wall shear stress $S(t)$ by resolving the convection diffusion equation. It was introduced by Beck *et al.* (1985) to solve heat transfer problems. Then Mao and Hanratty (1992) and Patankar (1980) used it to solve mass transfer problems. This method was well developed by Berrich (Berrich *et al.* 2011; Berrich *et al.* 2013a; Berrich *et al.* 2013b) for known simulated solutions of the convection-diffusion equation, and consists in the iterative determination of the wall velocity shear stress from the measured mass transfer. The flow sheet of this method is presented in Fig. 2. Starting from a guessed wall shear stress obtained using a classical method (Lévêque or transfer function), the convection diffusion equation is solved numerically to obtain mass transfer coefficient. The wall shear stress is then corrected and substituted in the convection diffusion equation, and new mass transfer coefficient is calculated. This process consists in the minimization of the difference between experimental data and the mass transfer coefficient obtained numerically thanks to the numerical inversion. The finite volume method with implicit scheme was applied by Beck *et al.* (1985). To spare the calculation time, resolution of the direct problem was optimized, and an optimization method was used in order to compress the calculation matrix of the convection-diffusion equation (Jeremy 1999; Markovic 1995). This allows to perform the method.

3. SETUP AND METHODS

An electrochemical cell consists of two electrodes (Fig. 3). The working electrode has a very small dimension to allow a local study of the mass transfer phenomena. The counter-electrode has a great dimension to have diffusion control on the working electrode only. The polarization voltage is chosen to obtain a diffusional plateau on current-voltage curves, which also corresponds to a zero where C_0 is the initial concentration of the reactive ion, As the active surface of the probe, the width of the rectangular probe, $\mathcal{D}$ the diffusion coefficient, $\mathcal{F}$ the Faraday number, n the number of electrons exchanged by a stoichiometric reaction and Sh the Sherwood number. The Sherwood number is a dimensionless number which is proportional to the rate (mass diffusivity/molecular diffusivity).

$$I = n.\mathcal{F}.C_0.A.\frac{\mathcal{D}}{l}.Sh \tag{7}$$

where Sh is defined by Eq. 4.

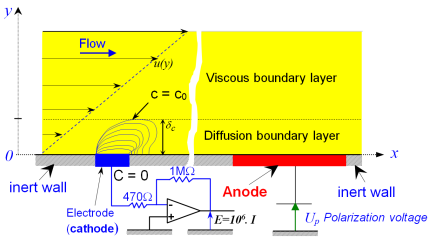

Fig. 3. Sketch of an electrochemical probe with its electronic circuit.

The wall-shear stress is experimentally determined using a $0.1mm \times 0.5mm$ rectangular electrode (Fig. 4) in a turbulent channel flow (Fig. 5). The electrolytic solution used is a mixture of ferri-ferrocyanide of potassium (10 mol/m^3) and potassium sulphate (240 mol/m^3). The chemical reaction at the electrodes is described by:

$$F_e(CN)_6^{4-} \rightleftharpoons F_e(CN)_6^{3-} + e^- \tag{8}$$

The limiting diffusion current was converted to voltage using a Keithley 6514 system electrometer, and acquired using a 12 bit A/D converter from an acquisition system Graphtec GL1000 that was controlled by a computer. The minimum sampling frequency was set above the u_τ^2/ν limit during 300 s for each measurement.

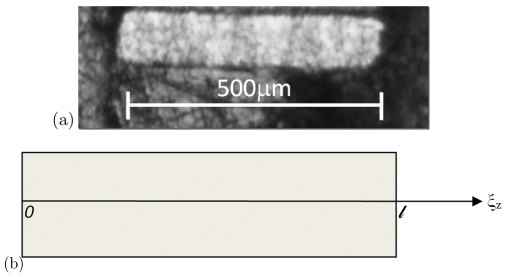

Fig. 4. Rectangular sensor used in this study to evaluate the fluctuating wall-shear stress: (a) Photography, (b) Detailed diagram.

The set-up originally designed for a turbulent boundary layer flow detailed in Lagraa *et al.* (2004), has been slightly modified to a channel flow configuration. For more information about the present experimental apparatus, see Keirsbulck *et al.* (2012). The dimensions of the channel cross-section are 150×10 mm, providing a 15 : 1 channel aspect ratio and the present measuring location was taken at a distance from the channel inlet of $125h$, where h denote the channel height. Full setup is shown in Fig. 5.

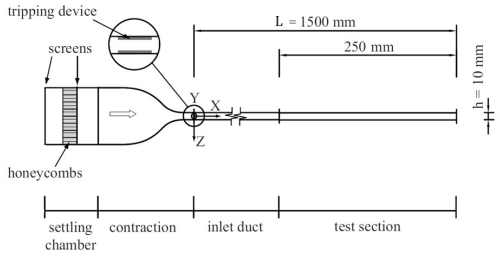

Fig. 5. Side view of the channel setup.

Very accurate evaluation of the relative wall shear stress fluctuation was sought after, consequently two correction processes must be made to ensure the quality of the wall statistics measurements. The first one is the frequency response correction of the electrochemical sensors and the second one is the spanwise correction of the non-uniformity flow over the electrode. We focus, on this second point and an important discussion will be made in the last part of this work. Considering the first point, Mao and Hanratty (1992) have developed a technique for the inverse problem, based on a numerical solution of the mass balance equation. More recently, the inverse method has been used by Rehimi *et al.* (2006) and also validated on transient flow (Zidouh *et al.* 2009; Berrich *et al.* 2011; Berrich *et al.* 2013a; Berrich *et al.* 2013b). The inverse method was applied in the present study for the determination of the "true" wall-shear stress fluctuations of the turbulent flow for different Kármán numbers ($Re_\tau = \frac{u_\tau . h/2}{\nu}$, where u_τ is the friction velocity). A typical time history of wall-shear stress with the quasi-steady assumption and using the inverse method are both plotted in Fig. 6 and have shown a significant increase in the wall-shear stress fluctuation when the inverse method is used.

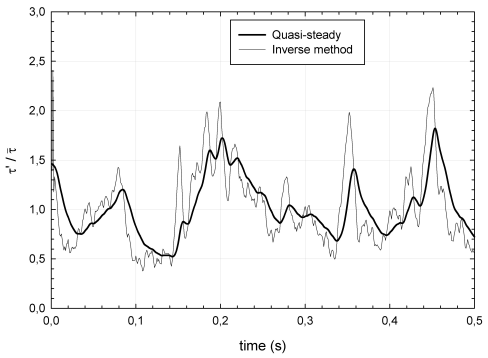

Fig. 6. Typical time history of wall-shear stress fluctuation using quasi-steady assumption and the inverse methods.

4. RESULTS AND DISCUSSION

In this paper, the study concerned firstly the correction method of the spatial averaging of the wall-shear stress fluctuations over the sensor surface leading to an underprediction of wall-statistics. As already mentioned by Alfredsson *et al.* (1988), it is also important to size down the sensors compared with the turbulence structures scale, so that local values of the fluctuating flow can be measured. Reiss and Hanratty (1963) suggested that turbulent velocity fluctuations close to a wall are dominated by flow structures featuring small spanwise dimensions and that are greatly elongated in the flow direction. These results suggest that spatial averaging in the flow direction is negligible but that, if the spanwise dimension of the probe is large compared to the spanwise dimension of the wall eddies, the assumption of a homogeneous flow over the probe surface will not be valid especially for high Kármán number. In order to take into account the spatial filtering effects on the wall-shear stress measurements due to the size of the wall-shear stress sensor, we proposed to extend the theoretical correction for non-uniform flow, introduced by Mitchell and Hanratty (1966). This formulation based on the spanwise correlation coefficient related to the eddy scaling methods recently suggested by Smits *et al.* (2011) for streamwise Reynolds

stress measurements close to the wall. The new formulation based on eddies concept seems to work very well for wall-bounded flows. Thus, for a rectangular electrode, the intensity of the wall-shear stress fluctuation can be corrected using the relationship originally proposed by Reiss and Hanratty (1963):

$$\frac{\overline{\tau_m'^2}}{\overline{\tau_r'^2}} = \frac{2}{l}\int_0^l (l-\xi_z)R(\xi_z)d\xi_z \tag{9}$$

where, l denotes the width of the rectangular electrode, R is the spanwise correlation coefficient and ξ_z, the transversal shift (Fig. 4b). Subscripts m and r denote the values measured and the real values respectively.

At this point, the development is somewhat arbitrary because of the necessity of introducing an assumption regarding the variation of the spanwise space correlation coefficient. The spanwise space correlation coefficient, defined bellow,

$$R(\xi_z) = \frac{\overline{\tau'(z)\tau'(z+\xi_z)}}{\sqrt{\overline{\tau'^2(z)}}\sqrt{\overline{\tau'^2(z+\xi_z)}}} \tag{10}$$

is plotted for different authors (Lagraa *et al.* (2004), Moser *et al.* (1999), Österlund (1999), Py (1990), Lee *et al.* (1974)) as a function of ξ_z^+ (Fig. 7), data from Lagraa *et al.* (2004) are in excellent agreement, especially with the correlation from Moser *et al.* (1999). The spanwise correlations reveal the existence of peaks, indicating that the quasi-streamwise structures were tilted in (x,z)-plane in accordance with the model suggested by Jeong *et al.* (1997). Knowledge of the streaks topology played a pivotal part in order to design suitable sensors that could be able to measure the wall-shear stress fluctuations with a sufficient accuracy. Assuming the spanwise space correlation shown in Fig. 7 to be independent of the Kármán number, we assume that the distribution $R(\xi_z^+) = exp(-(\frac{\xi_z^+}{\lambda^+})^2)$ fits correctly with the experimental and numerical data till $\xi_z^+ \approx 30$ with $\lambda^+ = 21$. This plot was used for the correction of the non-uniform flows, using Eq. 9 and the previous fit of the correlation, leading to the following expression of the correction coefficient for non-uniform flows:

$$\frac{\overline{\tau_m'^2}}{\overline{\tau_r'^2}} = \frac{1}{\alpha^2} = \frac{\lambda^+\sqrt{\pi}}{l^+} erf\left(\frac{l^+}{\lambda^+}\right) + \left(\frac{\lambda^+}{l^+}\right)^2\left[e^{-\left(\frac{l^+}{\lambda^+}\right)^2} - 1\right] \tag{11}$$

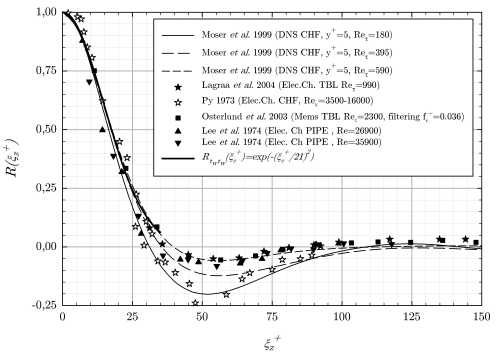

Fig. 7. Spanwise correlation coefficient against ξ_z^+ from experiments and DNS data. CHF indicates channel flow data, TBL, the turbulent boundary layer data and Elec. Ch, the electrochemical data.

The correction factors α of the relative wall-shear stress fluctuation due to the spanwise resolution are plotted in Fig. 8 and fit well with the spanwise filtering DNS Data from Örlü and Schlatter (2011).

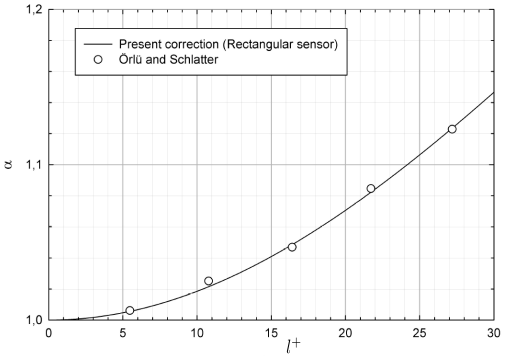

Fig. 8. Spanwise correlation coefficient against ξ_z^+ from experiments and DNS data.

The relative wall-shear stress fluctuation for different l^+ is reported in Table 1 with and without spanwise correction (frequency response correction are, for both cases, systematically applied). The measurements uncertainties on the relative wall-shear stress fluctuation are estimated to be equal to 0.02 (c subscript denotes the span correction and the DNS data obtained from Tsukahara *et al.* (2005)). Relative wall-shear stress fluctuation are in good agreement with the DNS values

when the spanwise correction is applied. But as mentioned by Örlü and Schlatter (2011), for a non-dimensional width $l^+ > 7$–8 wall units, the spanwise averaging effects are quite important as shown in Table 1. Abe *et al.* (2001) observed a similar decrease in the relative wall-shear stress fluctuation as a function of l^+. They found for $Re_\tau = 180$ an asymptotical value of the relative velocity fluctuation of 0.361 for $l^+ = 1.1$ and 0.359 for $l^+ = 4.5$. The present formulation is also of considerable interest from an experimental point of view and aims at explaining the seemingly discrepancy between experimental and numerical relative wall-shear stress results. The correction method proposed in the present study could be expanded to the velocity measurement and developed to remedy the turbulence intensity attenuation that occurs close to the wall as previously mentioned by Ligrani and Bradshaw (1987) using the corresponding velocity correlation and suitable λ parameter.

Table 1 Relative wall-shear stress fluctuation against the spanwise electrode dimension

	Elect.	DNS	Elect.	DNS
Re_τ	105	110	390	395
l^+	3.80	2.75	16.80	4.94
$\frac{\sqrt{\overline{\tau'^2}}}{\bar{\tau}}$	0.331	–	0.376	–
$\left(\frac{\sqrt{\overline{\tau'^2}}}{\bar{\tau}}\right)_c$	0.332	–	0.395	–
$\lim_{y^+\to 0} \frac{\sqrt{\overline{u'^{2+}}}}{U^+}$	–	0.335	–	0.398

5. CONCLUSION

The present paper attempts to put forward the electrochemical technique as an experimental methodology to contribute to the improvement of wall turbulence measurements and to propose a new correction formulation to take into account the spatial resolution effects for different sensors up to $l^+ \leq 30$. This correction method is base on the spanwise correlation function in order to take into account the non-uniform flow behavior observed for large spanwise sensors. In an experimental point of view, most of the sensor have a size less than l^+ of 30. Consequently, our present formulation seems to be of interest to improve the relative wall-shear stress fluctuation accuracy and to explain some of the discrepancy observed in the literature concerning this statistical quantity. The use of inverse method was important in this study to obtain the local and instantaneous "correct" wall shear stress. For the use of electrochemical measurement technique with higher fluctuations of the Sherwood number, all linear approaches create amplitude attenuation and phase shifts, and the inverse method remains the only good solution.

ACKNOWLEDGMENTS

The present research work has been supported by Campus International pour la Sécurité et l'Intermodalité des Transports, la Région Nord-Pas-de-Calais, l'Union Européenne, la Direction de la Recherche, Enseignement Supérieur, Santé et Technologies de l'Information et de la Communication et le Centre National de la Recherche Scientifique. The authors gratefully acknowledge the support of these institutions.

REFERENCES

Abe, H., H. Kawamura and Y. Matsuo (2001). Direct numerical simulation of a fully developed turbulent channel flow with respect to reynolds number dependence. ASME *J. Fluids Eng. 123*, 382.

Alfredsson, P., A. Johansson, J. Haritonidis and H. Eckelmann (1988). The fluctuating wall-shear stress and the velocity field in the viscous sublayer. *Phys. Fluids 31*(5), 1026.

Ambari, A., C. Deslouis and B. Tribollet (1985). Frequency response of mass transfer rate in a modulated flow at electrochemical probes. *Int. J. Heat Mass Transfer 29*, 35–45.

Beck, J., B. Blackwell and C. St-Clair (1985). Inverse heat conduction. *Wiley, New York*.

Berrich, E., F. Aloui and L. Legrand (2011). Inverse method for the dynamical analysis of wall shear rates using three-segment probes in parallel plate rheometer. *Chemical Engineering Science 66*, 3969–3978.

Berrich, E., F. Aloui and L. Legrand (2013a). Analysis of inverse method applied on sandwich probes. *Trans. of the ASME, Journal of Fluids Engineering 135*, 011401–1.

Berrich, E., F. Aloui and L. Legrand (2013b). Experimental validation and critical analysis of inverse method in mass transfer using electrochemical sensor. *Experimental Thermal and Fluid Science 44*, 253263.

Brücker, C., J. Spatz and W. Schröder (2005). Feasability study of wall shear

stress imaging using microstructured surfaces with flexible micropillars. *Exp. Fluids 39*, 464.

Buschmann, M. and M. Gad-el-Hak (2010). Normal and cross-flow reynolds stress: differences between confined and semi-confined flows. *Exp. Fluids 49*, 213.

Cameron, J. D., S. C. Morris, S. C. C.Bailey and A. J. Smits (2010). Effects of hot-wire length on the measurement of turbulent spectra in anisotropic flows. *Meas. Sci. Technol 21*, 105407.

Chantasiriwan, S. (1999). Comparison of three sequential function specification algorithms for the inverse heat conduction problem. *Int. Comm. in Heat Mass Transfer 26*, 115–124.

Chantasiriwan, S. (2001). An algorithm for solving multidimensional inverse heat conduction. *Int. Journal of Heat and Mass Transfer 44*(20), 3823–3832.

Chew, Y., B. Khoo, C. Lim and C. Teo (1998). Dynamic response of a hot-wire anemometer. part ii : A flush-mounted hot-wire and hot-film probes for wall shear stress measurements. *Measurement science and technology 9*(5), 764.

Degraaff, D. and J. Eaton (2000). Reynolds-number scaling of the flat-plate turbulent boundary layer. *J. Fluid Mech. 422*, 319.

Dumaine, J. (1981). Etude numérique de la réponse en fréquence des sondes électrochimiques. *Letters in Heat and Mass Transfer 8*, 293–302.

Durst, F., H. Kikura, I. Lekakis and J. Jovanović (1996). Wall shear stress determination from near-wall mean velocity data in turbulent pipe and channel flows. *Exp. Fluids 20*, 417.

Fischer, M., J. Jovanović and F. Durst (2001). Reynolds number effets in the near-wall region of turbulent channel flows. *Phys. Fluids 13*(6), 1755.

Hanratty, T. and J. Campbell (1996). Measurement of wall shear stress. *Fluid Mech. Measurements, second ed., Taylor and Francis, New York*, 559.

Hultmark, M., S. C. C. Bailey and A. J. Smits (2010). Scaling of near-wall turbulence in pipe flow. *J. Fluid Mech. 649*, 103.

Hutchins, N. and I. Marusic (2007). Evidence of very long meandering streamwise structures in the logarithmic region of turbulent boundary layers. *J. Fluid Mech. 579*, 1.

Hutchins, N., T. Nickels, I. Marusic and M. Chong (2009). Hot-wire spatial resolution issues in wall-bounded turbulence. *J. Fluid Mech. 635*, 103–136.

Jeong, J., F. Hussain, W. Schoppa and J. Kim (1997). Coherent structures near the wall in a turbulent channel flow. *J. Fluid Mech. 332*, 185.

Jeremy, G. (1999). A modern frame work for high performance linear algebra. *Master Thesis, University of Notre Dame, Department of Computer Science and Engineering, Indiana*.

Keirsbulck, L., L. Labraga and M. Gad-el-Hak (2012). Statistical properties of wall-shear-stress fluctuations in turbulent channel flows. *Int. J. Heat and Fluid Flow 37*, 1.

Lagraa, B., L. Labraga and A. Mazouz (2004). Characterization of low-speed streaks in the near-wall region of a turbulent boundary layer. *European Journal of Mech. B/Fluids 23*, 587.

Lee, M., L. Eckelman and T. Hanratty (1974). Identification of turbulent wall eddies through the pahse relation on the components of the fluctuating velocity gradient. *J. Fluid Mech. 66*, 17.

Ligrani, P. and P. Bradshaw (1987). Spatial resolution and measurement of turbulence in the viscous sublayer using subminiature hot-wire probes. *Exp. Fluids 5*, 407.

Ling, S. (1963). Heat transfer from a small spanwise on an insulated boundary. *J. Heat transfer, Trans. ASME*, 230–236.

Mao, Z. and T. Hanratty (1991). Analysis of wall shear stress probes in large amplitude unsteady flows. *Int. J. Heat Mass Transfer 34*, 281–290.

Mao, Z. and T. Hanratty (1992). Measurement of wall shear rate in large amplitude unsteady flows. *Exp. Fluids 12*, 342–350.

Markovic, A. (1995). An investigation of sparse matrix solvers with applications to models of transport in porous media. *Master in sciences, Center in statistical science and industrial mathematics, Queensland University of Technology*.

Örlü, R., J. Fransson and P. Alfredsson (2010). On near wall measurements of wall bounded flows-the necessity of an accurate determination of the wall position. *Prog. Aerospace Sci.J. Fluid Mech. 46*(8), 353.

Örlü, R. and P. Schlatter (2011). On the fluctuating wall-shear stress in zero pressure-gradient turbulent boundary layer flows. *Phys. Fluids 23*(0211704).

Österlund, J. (1999). Experimental studies of zero-pressure-gradient turbulent boundary layer flow. *Ph.D. thesis, Royal Institute of Technology*.

Mitchell, J. and T. Hanratty (1966). A study of turbulence at a wall using an electrochemical wall shear stress meter. *J. Fluid Mech. 26*, 199.

Miyagi, N., M. Kimura, H. Shoji, A. Saima, C. Ho, S. Tung and Y. Tai (2000). Statistical analysis on wall-shear stress of turbulent boundary layer in a channel flow using micro-shear stress imager. *Int. J. Heat Fluid Flow 21*, 576.

Monkewitz, P. A., R. D. Duncan and H. M. Nagib (2010). Correcting hot-wire measurements of stream-wise turbulence intensity in boundary layers. *Phys. Fluids 22*, 091701.

Monty, J., N. Hutchins, H. Ng, I. Marusic and M. Chong (2009). A comparison of turbulent pipe, channe and boundary layer flows. *J. Fluid Mech. 632*, 431.

Monty, J., J. Stewart, R. William and M. Chong (2009). Large-scale features in turbulent pipe and channel flows. *J. Fluid Mech. 589*, 147.

Morrison, J., B. McKeon, W. Jiang and A. Smits (2004). Scaling the streamwise velocity component in turbulent pipe flow. *J. Fluid Mech. 508*, 99.

Moser, R., J. Kim and N. Mansour (1999). Direct numerical simulation of a turbulent channel flow up to $\mathrm{Re}_\tau = 590$. *Phys. Fluids 11*, 943.

Naqwi, A. and W. Reynolds (1991). Measurement of turbulent wall velocity gradients using cylindrical waves of laser light. *Exp. Fluids 10*, 257.

Patankar, S. (1980). Numerical heat transfer fluid flow. *Hemisphere/ Mc Graw-Hill, New York*.

Py, B. (1990). Improvement in the frequency response of the electrochemical wall shear stress meter. *Exp. Fluids 8*, 281.

Rehimi, F., F. Aloui, S. Ben Nasrallah, L. Doubliez and J. Legrand (2006). Inverse method for electrodiffusional diagnostics of flows. *Int. J. Heat Mass Transfer 49*, 1242.

Reiss, L. and T. Hanratty (1963). An experimental study of the unsteady nature of the viscous sublayer. *A.I.Ch.E. J. 9*, 154.

Segalini, A., R. Örlü, P. Schlatter, P. Alfredsson, J. Rüedi and A. Talamelli (2013). A method to estimate turbulence intensity and transverse taylor microscale in turbulent flows from spatially averaged hot-wire data. *Experiments in Fluids 51*, 693–700.

Smits, A., J. Monty, M. Hultmark, S. Bailey, N. Hutchins and I. Marusic (2011). Spatial resolution correction for wall bounded turbulence measurements. *J. Fluid Mech. 676*, 4153.

Sobolik, S., O. Wein and J. Cermak (1987). Simultaneous measurement of film thickness and wall shear stress in wavy flow of non-newtonian liquids. *Coll. Czech. Chem. Commun. 52*, 913.

Sobolik, V., P. Mitschka and T. Menzel (1986). Method of manufacture of segmented probe with circular cross-section. *Czechoslovak Pat. AO*, 262–823.

Talamelli, A., A. Segalini, R.Örlü, P. Schlatter and P. Alfredsson (2013). Correcting hot-wire spatial resolution effects in third- and fourth-order velocity moments in wall-bounded turbulence. *Experiments in Fluids 54(4)*, 1–11.

Tihon, J., J. Legrand and P. Legentilhomme (1995). Dynamics of electrodiffusion probes in developing annular flows. *Exp. Fluids 20*(2), 131–134.

Tortorelli, D. and P. Michaleris (1994). Design sensitivity analysis: Overview and review. *Inverse Problems in Engineering*, 71–105.

Tsukahara, T., Y. Seki, Kawamura and D. Tochio (2005). DNS of turbulent channel flow at very low reynolds numbers. *In Proc. of the Forth Int. Symp. on Turbulence and Shear Flow Phenomena, Williamsburg,* USA, 935.

Wu, X. and P. Moin (2010). Transitional and turbulent boundary layer with eat transfer. *Phys. Fluids 22*, 085105.

Zidouh, H., L. Labraga and M. William-Louis (2009). Unsteady wall shear stress in transient flow using electrochemical method. *J. Fluids engineering 131*(5).